Unit cells for multiphysics modelling of structural battery composites

(article starts on next page)

UNIT CELLS FOR MULTIPHYSICS MODELLING OF STRUCTURAL BATTERY COMPOSITES

David Carlstedt[1*], Johanna Xu[1], Kenneth Runesson[1], Fredrik Larsson[1] and Leif E. Asp[1]

[1] Department of Industrial and Materials Science, Chalmers University of Technology, Gothenburg, Sweden, *david.carlstedt@chalmers.se

ABSTRACT

To predict the multifunctional performance of structural battery composites, multiple physical phenomena need to be studied simultaneously. Hence, multiphysics models are needed to evaluate the complete performance of this composite material. In this study the coupled analysis for multiphysics modelling of structural battery composites is presented and modelling strategies and unit cell designs are discussed with respect to the different physical models. Furthermore, FE-models are setup in the commercial Finite Element (FE) software COMSOL to study if existing physics-based modelling techniques and homogenization schemes for conventional lithium ion batteries can be used to describe the electrochemical behaviour of structural battery composites. To predict the microscopic behaviour, the local variation of the mass and charge concentrations need to be accounted for. Hence, refined models with appropriate boundary conditions are needed to capture the microscopic conditions inside the material. The numerical results demonstrate that conventional physics-based 1D battery models and homogenization schemes based on porous media theory can be used to predict the macroscopic electrical behaviour of the fibrous structural battery. For future work electrochemical experiments on battery cell level are planned to validate the numerical results.

1 INTRODUCTION

The structural battery is a composite material made from carbon fibre reinforced polymer. This multifunctional composite material has the ability to carry mechanical loads while storing electrical energy. Two types of structural battery composite architectures have been proposed. The first one is the laminated battery architecture. This was first proposed by Wetzel et al. [1] and later demonstrated by Ekstedt et al. [2] and Carlson [3]. In this design the individual laminae have separate functions and work as electrode, separator, current collector, etc. The second one was developed by Asp and co-workers [3-5] and is often referred to as the 3D (or Micro) battery architecture. In this design the individual fibres are coated with thin polymer electrolyte coating before they are placed inside a polymer matrix doped with positive electrode particles. State-of-the-art versions of the two battery architectures are schematically illustrated in Figure 1.
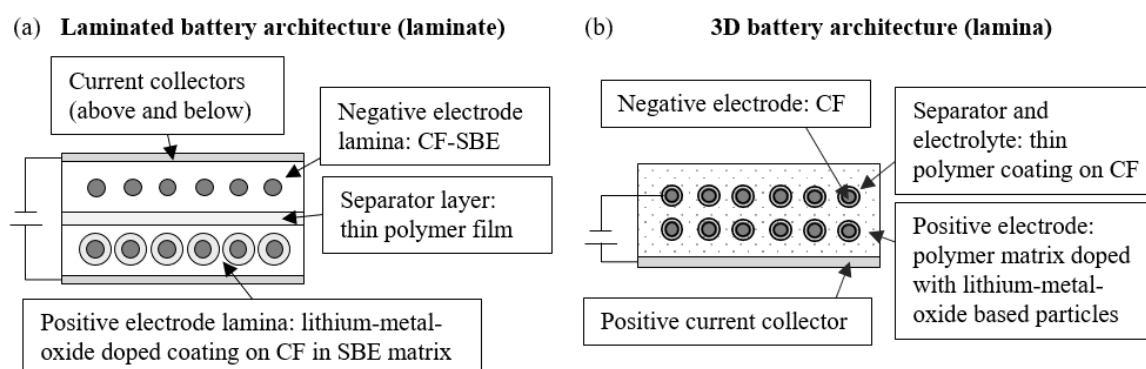

Figure 1: Schematic illustrations of the structural battery composite architectures (CF=carbon fibre, SBE=Structural battery electrolyte). a) laminated battery. b) 3D battery.

In both designs the fibres in the composite laminae work as active electrode material (hosts for the lithium) and/or current collectors. Previous studies [6-7] have shown high specific mechanical and electrical properties of carbon fibres which indicate that they are ideal for multifunctional application. Moreover, the work by Johannisson et al. [8] on laminated structural battery negative half-cells demonstrates the maturity of this design and suggests highly promising multifunctional performance of this material.

To evaluate the performance of this material using computational models, multiple physical phenomena need to be considered simultaneously. Hence, multiphysics models are needed to evaluate the complete multifunctional performance. As the structural battery composite is intended to carry mechanical loads while working as a battery, the coupling of the mechanical and electrical response is of importance. In addition, the mechanical and electrical response are highly affected by the temperature. This means that thermal effects need to be accounted for and coupled to the mechanical and electrochemical models.

In earlier work on computational modelling of structural battery composites standard unit cells for mechanical analysis of UD fibre reinforced polymer composites have been used to study the material performance. In the work done by Xu et al. [9-10], a numerical framework using a multiphysics FE-model was developed to study how the internal stresses in 3D structural batteries are affected by volume change of constituents. In these studies, mechanical-electrical coupled analysis was performed using concentric cylinder unit cells. Moreover, in the work by Carlstedt et el. [11-12] the mechanical consequences of electrochemical cycling were studied by simplifying the electrochemical and thermal processes to allow for the use of standard micromechanical models for mechanical analysis such as concentric cylinder models and repeatable unit cells representing square and hexagonal packing. In all these studies, the analysis is one-way where the electrochemical and thermal analysis are used to derive input data to the mechanical analysis.

In previous work by the authors [9-12] the lithium (Li) concentration distribution inside the fibres was shown to have a significant effect on the internal stress state. In these studies, the current was assumed to be extracted on the boundary of the unit cell which results in a one-dimensional lithium concentration distribution that is equal for each unit cell. Therefore, as a next step towards solving the complete multiphysics problem the mass and charge transport problems, related to the electrochemical analysis, need to be studied under relevant boundary conditions. Depending on which of the structural battery composite architectures (Figure 1) that is evaluated different boundary conditions are required. One potential route to solve the mass and charge transport problem inside the structural battery is to use existing modelling techniques and homogenization schemes [13-14] for ordinary lithium ion batteries. The applicability of such macroscopically homogenous models for modelling ordinary lithium ion batteries has been studied previously [15-16]. To date no study exists to evaluate if existing battery models can be used to predict the electrochemical behaviour of structural battery composites.

In this work the coupled analysis for multiphysics modelling of structural battery composites is presented and discussed. Furthermore, modelling strategies and unit cell designs are discussed with respect to the different physical models. To evaluate if existing physics-based modelling techniques and homogenization schemes [13-14] for ordinary lithium ion batteries can be used for structural battery composites FE-models are setup in the commercial Finite Element (FE) software COMSOL. To limit the scope of the current paper, only the laminated structural battery architecture (Figure 1a) is studied. Moreover, to simplify the model and the experimental validation (future work) only the negative electrode laminae (upper lamina in Figure 1a) is resolved and properties for conventional liquid electrolyte are used.

2 COUPLED ANALYSIS FOR STRUCTURAL BATTERY COMPOSITES

A schematic illustration of the coupled analysis for structural battery composites is presented in Figure 2. The essential couplings between the physical domains are illustrated as arrows between each box in Figure 2 where T is the temperature field, c is the lithium concentration in the active electrode materials, ε is the mechanical strain, Q_E is the generated heat due electrochemical effects and Q_D is the heat generated due to energy dissipation (related to mechanical work).
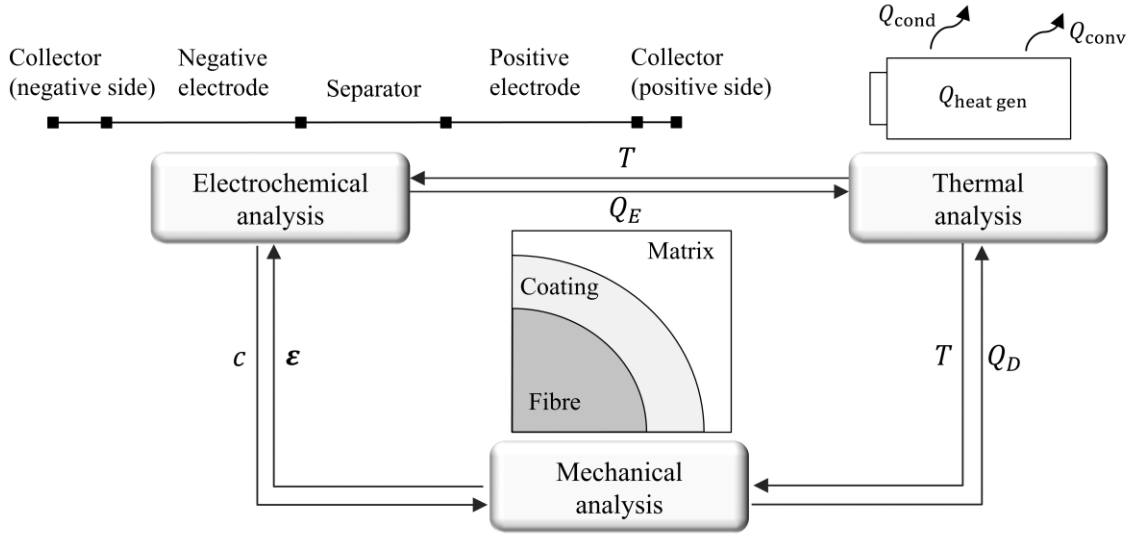

Figure 2: Schematic illustration of the coupled analysis in the multiphysics model.

To estimate the electrical performance, related to the battery functionality of this material, electrochemical analysis needs to be performed. This analysis allows for estimation of the electrical performance of the material related to electrical power, current, etc. During electrochemical cycling heat is generated or absorbed (Q_E) and the lithium concentration in the active electrode materials (c) is altered. It has been shown that the volume and elastic properties of electrode materials such as carbon fibres and positive electrode particles are affected by lithium-ion (Li^+) concentration [17-18]. This means that the battery functionality is coupled with the thermal and mechanical analysis. Moreover, mechanical strains (ε) will affect the electrochemical process e.g. due to closing of pores, mechanical fracture of constituents, etc. and energy dissipation will generate heat (Q_D). The temperature distribution inside the material and heat exchange with the surroundings (T) will affect both the mechanical and electrical performance. Hence, to estimate the complete performance of the material with respect to the different physical phenomena refined modelling techniques that allow for couplings of the different physical models are required. Due to the different nature of the considered physical problems different modelling techniques are often used to solve the respective problems. In the following section modelling strategies and unit cells designs are discussed with respect to the different analyses.

2.1 Electrochemical analysis

Numerous mathematical models to study the electrochemical behaviour of lithium-ion batteries are available in literature. Depending on the purpose of the model, the formulations differ significantly. Physics-based models are most useful, when the electrochemical processes are of interest. These models consist of mathematical formulations in the form of differential equations describing the physical battery features in space and time. Figure 3 shows a schematic illustration of the internal structure of an ordinary lithium ion battery cell. In conventional lithium ion batteries, the active electrode materials in the electrodes are graphite and Li-based particles in the negative and positive electrode, respectively. Furthermore, conductive additives are added in both electrodes to enhance their electrical conductivities and liquid electrolyte is used to enable ion-transport between the electrodes inside the cell.
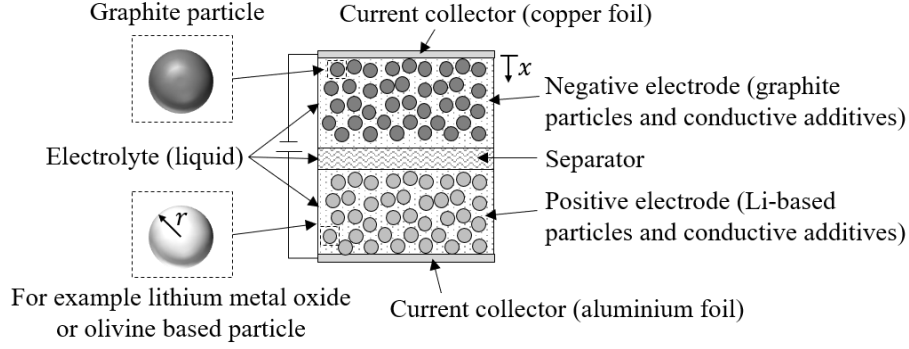
Figure 3: Schematic illustration of the internal structure of an ordinary lithium ion battery cell.

In electrochemical analysis of batteries, one-dimensional (also known as pseudo-two-dimensional) models are often used to evaluate the electrical performance of the studied battery. These models are based on the work by Newman and co-workers [13-14] assuming homogenized properties of the porous structure of the battery constituents (electrodes and separator). In this framework the processes occurring during electrochemical cycling can be described based on the governing equations for the mass and charge transport problem in the different phases (solid and liquid phase). These equations are presented in the following. For simplicity we only report the governing equations for the case of a one-dimensional current/mass flow inside the battery cell.

2.1.1 Solid phase (active electrode and conductive materials in electrodes)

The charge balance in the solid phase is governed by Ohm's law and reads

$$\frac{\partial}{\partial x}\left(\hat{s}\frac{\partial \varphi_s}{\partial x}\right) = i_{\mathrm{loc}}a \tag{1}$$

where $\hat{s}$ is the effective electrical conductivity and φ_s is the electrical potential in the solid phase (fibres and particles). In Eq. (1) i_{loc} is the average current density at the electrode surface defined by the Butler-Volmer kinetics expression [13]. Moreover, a is the volume specific interfacial area (m^{-1}) which depends on the shape of the electrode material. This area can be approximated as $a = kV_s/r_s$ where $k=3$ for spherical particles and $k=2$ for cylinders. The volume fraction of the electrode materials (solid phase) is denoted V_s and correspond to the volume fraction of fibres (V_f) and particles (V_p) in the negative and positive electrode, respectively. The radius of the inclusions is denoted r_s (fibre r_f and particle r_p).

2.1.2 Liquid phase (electrolyte in electrodes and separator)

The material balance for the electrolyte (liquid phase) reads

$$\frac{\partial V_e c_e}{\partial t} = \frac{\partial}{\partial x}\left(\widehat{D}_e \frac{\partial c_e}{\partial x}\right) + \frac{(1-t_+)}{F} i_{\mathrm{loc}}a \tag{2}$$

where V_e is the volume fraction of the electrolyte in the electrode/separator, c_e is the lithium salt concentration in the electrolyte phase, $\widehat{D}_e$ is the effective diffusion coefficient of lithium ions in the electrolyte, t_+ is the transport number of Li$^+$ (describing the fraction of electrical current carried by the ionic specie) and F is Faraday's constant. Finally, the charge balance in the electrolyte (also governed by Ohm's law) can be expressed as

$$-\frac{\partial}{\partial x}\left(\hat{\kappa}_e \frac{\partial \varphi_e}{\partial x}\right) + \frac{2RT(1-t_+)}{F}\frac{\partial}{\partial x}\left(\hat{\kappa}_e \frac{\partial \ln(c_e)}{\partial x}\right) = i_{\mathrm{loc}}a \tag{3}$$

where $\hat{\kappa}_e$ is the effective ion conductivity of the electrolyte and φ_e is the electrolyte potential. The governing equations are solved with respect to the applied boundary conditions. In the 1D-model Eq. (1)–(3) are defined with respective to a one dimensional coordinate system (x) in the through thickness direction of the battery cell (Figure 3).

2.1.3 Charge transfer (between electrolyte and active electrode materials)

The kinetics for the charge-transfer process at the electrode surface is described using a Butler-Volmer type kinetic expression [13] defined as

$$i_{\text{loc}} = i_0 \left(\exp\left(\frac{\alpha_a F \eta}{RT}\right) - \exp\left(-\frac{\alpha_c F \eta}{RT}\right) \right) \tag{4}$$

where i_0 is the exchange current density (defined as stated in e.g. [13]), T is the temperature, R is the universal gas constant (8.314 J K^{-1}mol^{-1}) and α_a, α_c are the electrochemical reaction symmetry factors for the anodic and cathodic reactions, respectively. This equation describes the process of charge-transfer between the electrolyte (liquid phase) and the active electrode materials (solid phase). The surface overpotential is defined as $\eta = \varphi_s - \varphi_e - E_{\text{eq}}$, where E_{eq} is the equilibrium potential of the electrode. By combining Eq. (1)–(4) and imposing relevant boundary conditions [13] it is possible to solve for the mass and charge distribution inside the cell.

2.1.4 Mass transport inside active electrode material

The material balance for the lithium in the electrode particles or fibres (solid phase) are governed by Fick's second law and reads

$$\frac{\partial c_s}{\partial t} = \frac{1}{r^\alpha} \frac{\partial}{\partial r} \left(D_s r^\alpha \frac{\partial c_s}{\partial r} \right) \tag{5}$$

where c_s is the lithium concentration in the solid phase and D_s is the diffusion coefficient of Li in the solid phase. The diffusion problem in Eq. (5) is defined for spherical ($\alpha = 2$) and cylindrical ($\alpha = 1$) coordinates for particles and fibres, respectively, with respect its radial dimensional (illustrated for the positive electrode particle in Figure 3). By imposing boundary conditions related to the current/mass flow between electrolyte (liquid phase) and the active electrode materials (solid phase), cf. Eq. (4), the lithium distribution inside the active electrode material can be resolved. It should be noted that Eq. (1)-(3) and Eq. (5) are defined in different (unrelated) dimensions. For this reason, this type of model is often referred to as a pseudo two-dimensional model.

2.1.5 Effective properties

In the work by Newman and Tiedemann [13] a homogenization scheme for porous electrodes in battery application was developed based on earlier work by Bruggeman [19]. In this framework the effective mass and charge transport properties are derived using power law equations based on the volume fraction and tortuosity of the system. These properties are defined as

$$\widehat{D}_j = D_i V_i^\beta \tag{6}$$

$$\hat{s}_j = s_i V_i^\beta \tag{7}$$

$$\hat{\kappa}_j = \kappa_i V_i^\beta \tag{8}$$

where j corresponds to the battery component (electrodes and separator) and i corresponds to the transporting constituent (electrolyte and fibres/particles). The Bruggeman's constant (linked to the tortuosity) is denoted β.

2.2 Mechanical analysis

For mechanical analysis of composite materials repeatable unit cells (RUC) representing square and hexagonal packing arrangement or concentric cylinders are often used to predict effective elastic properties and to study internal stresses in composite materials. In Figure 4 RUCs representing square and hexagonal packing arrangement set-up in the commercial FE software COMSOL 5.3a are presented. These models have been used in earlier work by the authors [11] to estimate the effective elastic properties of 3D structural battery composites (Figure 1b).
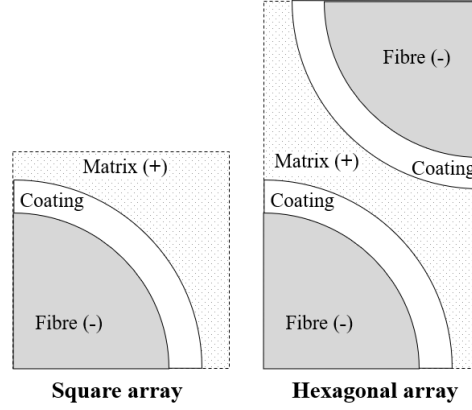
Figure 4: Computational models set-up in the commercial FE software COMSOL 5.3a for square and hexagonal fibre packing, respectively, used to estimate effective elastic properties of 3D structural battery composites [11].

It is also common to use representative volume elements (RVEs) that account for the random variation of fibres [20]. Both the RUC and RVE are commonly used to represent the smallest volume of a repeatable structure with respect to the structural performance and can be used to estimate the effective elastic properties and internal stress state in composite materials. Hence, the mechanical performance of the structural battery composite can be assessed utilizing standard micromechanical models projecting the microscale problem to the macroscale using a suitable homogenization scheme. The governing equation for the quasi-static mechanical problem is defined based on momentum balance as

$$-\boldsymbol{\sigma} \cdot \boldsymbol{\nabla} = 0 \tag{9}$$

where $\boldsymbol{\sigma}$ is the (symmetric) stress tensor and the body load is set to zero (no external load). In previous work by the authors [9-10,12] the stress distribution inside the electrodes have been resolved by linking the change in lithium distribution inside the active electrode material (cf. Eq. (5)) with changes in volume and stiffness of the constituents.

2.3 Thermal analysis

In the thermal analysis the heat distribution and heat transfer, within and between the domains, are estimated. These effects are governed by the thermal energy balance which can be expressed as

$$mC_{\mathrm{p}} \frac{\partial T}{\partial t} = Q_{\mathrm{gen}} + Q_{\mathrm{ext}} \tag{10}$$

where m is the mass, C_{p} is the specific heat, Q_{gen} is the generated heat and Q_{ext} is the heat exchange with the surroundings. For thermal modelling of batteries lumped parameter models are often used [21]. In these models the total generated heat inside the battery is assumed to be a summation of the heat generated inside the individual constituents. In earlier work by the authors [12] a lumped parameter model was developed to estimate the change in temperature in a 3D structural battery due to heat generation during galvanostatic cycling (constant current charge/discharge). In this work the ohmic heat inside the battery cell was estimated based on the applied current and the equivalent resistance of a number of resistors (representing the current flow in each phase) connected in series.

Due to the thermal sensitivity of the electrochemical processes [21], it is crucial to accurately resolve the temperature field inside the structural battery. Moreover, the mechanical performance of composite materials is highly affected by temperature. This means that heat generation and heat transport conditions need to be properly set-up with respect to the given boundary conditions in the thermal model to predict the temperature variation inside the material during operation.

3   BATTERY MODELLING

To evaluate if existing physics-based modelling techniques and homogenization schemes [13-14] for ordinary lithium ion batteries can be used for structural battery composites two FE-models are setup in the commercial Finite Element (FE) software COMSOL 5.3a. The model geometries of the two models are presented in Figure 5.
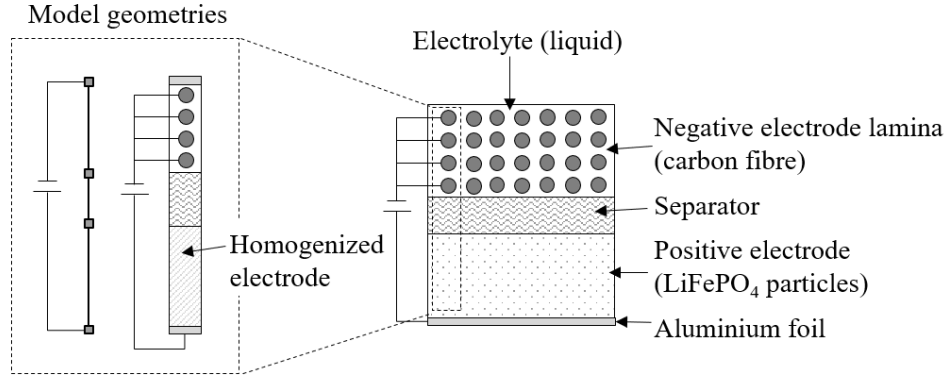

Figure 5: Model geometries for electrochemical analysis of the structural battery.

The negative electrode is assumed to be made of a carbon fibre embedded in liquid electrolyte. Moreover, the positive electrode is assumed to be made of LiFePO$_4$ particles adhered to an aluminium foil (i.e. a commercial positive electrode). The liquid electrolyte is assumed to be 1.0 M LiPF$_6$ in EC:DEC 1:1 w/w (LP40 Aldrich) electrolyte. This corresponds to a commercially available electrolyte used in conventional lithium ion batteries. The carbon fibres in the negative electrode lamina and the particles in the positive electrode lamina are the active electrode materials (host for lithium) in the battery cell. The developed models are used to study the following two cases: (i) 1D-model assuming homogenized properties of the complete battery lamina and (ii) 2D model where the carbon fibres in the negative electrode lamina are modelled explicitly. The 1D model corresponds to standard model for ordinary lithium ion batteries assuming a one-dimensional current flow between the collectors inside the cell. In the 2D model the fibres are modelled explicitly in the negative electrode while effective (homogenized) properties are used for the positive electrode. The two FE-models are presented in Figure 6.
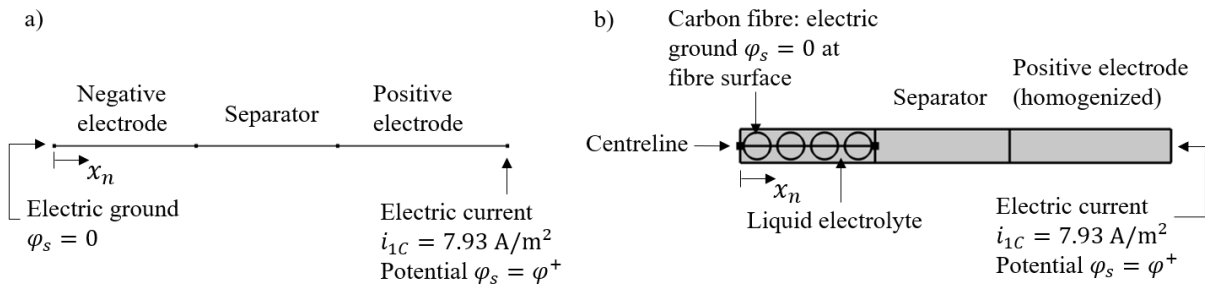

Figure 6: Electrochemical models set-up in the commercial FE software COMSOL 5.3a. (a) 1D model with homogenized properties. (b) 2D model with electrode materials (fibres) explicitly modelled in negative electrode lamina.

The geometric parameters of the model are summarised in Table 1 and the assumed model properties are listed in Appendix A. The negative electrode is assumed to have a thickness that corresponds to four fibres in the thickness direction. The separator is assumed to be made of a 25 µm thick ceramic-reinforced non-woven polyester separator.

Geometric parameter	CF–SBE lamina (negative electrode)	Separator	Positive electrode
Thickness (μm)	25	25	30
Radius of electrode materials (μm)	$r_f = 2.5$	-	$r_p = 0.1$

Table 1: Model geometry.

For the studied case a constant current is applied (i.e. galvanostatic cycling). This current is set to 7.93 A/m² which corresponds to a C-rate of approximately 0.7 (i.e. with this current it takes 0.7 hour or 42 min to fully charge or discharge the battery). The cut-off limit is set to 2.8 V. Under these conditions the potential difference between the poles will vary during charge/discharge. Hence, the driving force will depend on the potential difference between the electrodes at the given time. Furthermore, isothermal conditions are assumed (room temperature) and the equilibrium potential for the carbon fibres are based on measurements made by Kjell et al. [24]. The potential curve for the LiFePO₄ particles is taken from the COMSOL library. For simplicity the electrolyte conductivity and diffusivity are assumed not to be affected by changes in salt concentration.

4   RESULTS AND DICSUSSIONS

The electrical performance is derived by solving the governing equations for the electrochemical analysis presented in section 2.1 using COMSOL. In Figure 7 the potential curve during discharge for the two models are presented.
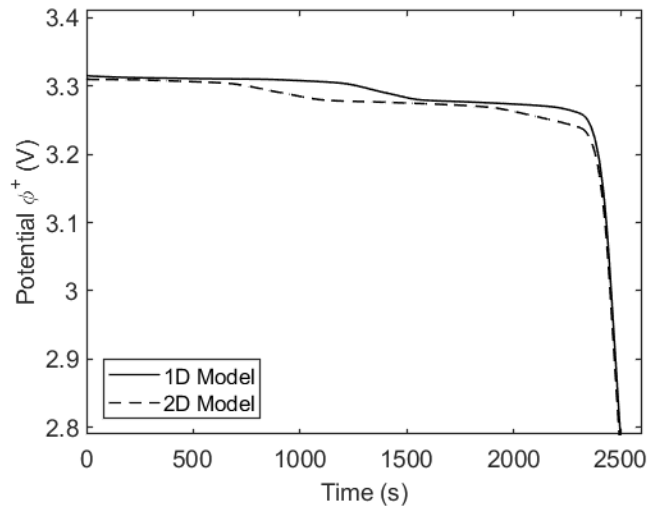

Figure 7: (a) Potential curve during discharge for the two models.

The overall behaviour of the potential curves for the two models are similar (Figure 7). This means that the two models predict similar overall electrical performance related to battery power output (macroscopic behaviour). Compared with ordinary batteries, the active electrode materials in the structural battery are intended to carry mechanical load. As the lithium concentration inside the material affects the elastic properties and volumes of the constituents it is important to be able to accurately resolve the lithium distribution inside the battery cell to predict the internal stress state. In Figure 8 the lithium concentration distribution inside the negative electrode for the two models are presented. The concentration distribution is plotted at three time instances ($t_1 = 100$ s, $t_2 = 1100$ s and $t_3 = 2100$ s) during discharge.
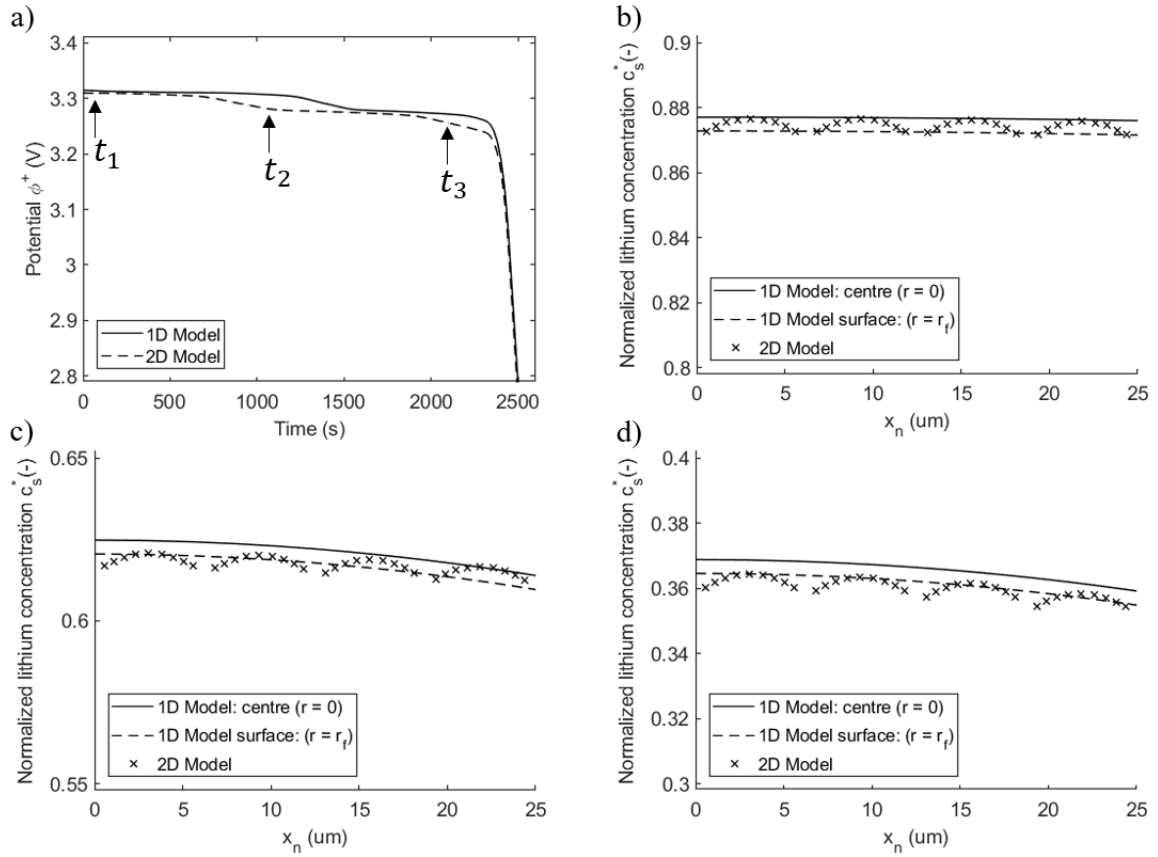
Figure 8: (a) The three time instances (t_1, t_2 and t_3) when the lithium concentration is plotted indicated in the potential curve. The normalized lithium concentration ($c_s{}^* = c_f / c_{f,\max}$) in the fibres in the negative electrode at (b) $t_1 = 100$ s (c) $t_2 = 1100$ s and (d) $t_3 = 2100$ s. For the 1D model the concentration is plotted at the fibre centre and surface, respectively while the concentration inside the 2D model is plotted along the centreline (Figure 6b).

In Figure 8 the lithium concentrations at the fibre centre ($r = 0$) and surface ($r = r_f$) are plotted for the 1D model while the concentration inside the 2D model is plotted along the centreline (Figure 6b). The variation in the distribution perpendicular to the centreline in the 2D model is not presented. This variation was found small for the studied case but is highly dependent on the transport properties of the constituents. It should be noted that the lithium distribution in the 2D model varies for different sections and that it is influenced by the assumed packaging arrangement (unit cell design). The difference in the lithium concentration between the two models however indicates that the microscopic behaviour is different for the two models. Hence, the microscopic consequences e.g. related to the local variation in lithium concentration (affecting the internal stress state) is affected by the assumptions of the models. The average lithium distribution inside the negative electrode on the other hand is similar for the two models (Figure 8) which indicates that the macroscopic behaviour of the cell is similar (as previously discussed). In this analysis, the electrolyte is assumed to be made of commercial liquid electrolyte for ordinary lithium ion batteries. The transport properties of the electrolyte have significant effect on the mass transport inside the battery cell. For example, the ion conductivity of structural battery electrolytes (SBE) used in structural batteries have been reported in the range of 10^{-4} S/cm [22] while the conductivity of ordinary liquid electrolytes often is in the range 10^{-2}–10^{-3} S/cm [23]. This means that the electrolyte properties and the thickness of the different layers will have a significant effect on the electrical performance. Due to the coupling of the physical phenomena, this will also influence the internal stress state inside the material and the temperature generation. Hence, as future work the transportation properties of the SBE need to be determined and included in the model.

5 CONCLUSIONS

To evaluate the performance of structural battery composites using computational models, multiple physical phenomena need to be studied simultaneously. Hence, multiphysics models are needed to evaluate the multifunctional performance of this composite material. In this study the coupled analysis for multiphysics modelling of structural battery composites are presented and discussed. Furthermore, modelling strategies and unit cell designs are discussed with respect to the different physical models.

As a next step towards solving the complete multiphysics problem, the mass and charge transportation problem (related to the electrochemical analysis) needs to be studied for representative geometries and boundary conditions. A potential route to solve this problem is to use existing physics-based modelling techniques and homogenization schemes for ordinary lithium ion batteries. To study if these modelling techniques and homogenization schemes can be used to predict the electrochemical behaviour of structural battery composites FE-models were setup in the commercial Finite Element software COMSOL. To limit the scope of the study, only the laminated structural battery architecture was studied. Moreover, only the negative electrode laminae, assumed to be made of carbon fibres embedded in liquid electrolyte was resolved at this stage to simplify the models and the experimental validation in future work. Two types of models were set-up in COMSOL. The first model was a 1D model (pseudo-2D) assuming homogenized properties of the complete battery lamina. This corresponds to the conventional physics-based model for ordinary lithium ion batteries assuming a one-dimensional current flow between the collectors inside the cell. The second model was a 2D model where the fibres were modelled explicitly in the negative electrode.

For the studied case the overall electrical performance related to battery power output (macroscopic behaviour) was found to be similar for the two cases. To capture the microscopic behaviour, related to the lithium concentration distributions, the local variations need to be accounted for. Hence, refined models with appropriate boundary conditions (such as the 2D model) are needed to capture the local variation of e.g. the lithium concentration inside the material. For future work, electrochemical experiments on battery cell level and characterization of constituents are planned. These experiments will be used to validate the models and to provide additional input data needed to predict the electrical performance of the structural battery composites.

APPENDIX A

Parameter	Value	Unit	Description	Source
I_{app}	7.93	[A/m^2]	Applied discharge current density	Calculated
V_p, V_f	0.4, 0.5	[-]	Volume fraction of LiFePO$_4$ particles positive electrode (p) and fibres in negative electrode (f)	
V_e	0.5	[-]	Volume fraction of electrolyte in positive electrode, negative electrode and separator	
D_e	$1 \cdot 10^{-10}$	[m^2/s]	Liquid phase Li$^+$-diffusivity electrolyte	
D_p	$3.2 \cdot 10^{-13}$	[m^2/s]	Solid phase Li-diffusivity LiFePO$_4$ particles	
D_f	$1.0 \cdot 10^{-13}$	[m^2/s]	Solid phase Li-diffusivity carbon fibre	[24]
r_p	0.1	[μm]	Radius of LiFePO$_4$ particle	
r_f	2.5	[μm]	Radius of carbon fibre	
α_a, α_c	0.5, 0.5	[-]	Anodic and cathodic transfer coefficients (both electrodes)	
β	1.5	[-]	Bruggeman constant (for all phases)	
t_+	0.364	[-]	Transport number of Li$^+$	
i_0	1	[A/m^2]	Exchange current density (both electrodes)	
κ_e	0.8	[S/m]	Ion conductivity electrolyte	
$\tilde{s}_p$	91	[S/m]	Electronic conductivity solid phase in positive electrode (LiFePO$_4$ and conductive additives)	
s_f	69000	[S/m]	Electronic conductivity carbon fibre	[24]
$c_{e,ini}$	1000	[mol/m^3]	Initial salt concentration in electrolyte	
$c_{p,ini}$	2270	[mol/m^3]	Initial lithium concentration LiFePO$_4$ particles	
$c_{f,ini}$	23110	[mol/m^3]	Initial lithium concentration carbon fibres	
$c_{p,max}$	22700	[mol/m^3]	Max. lithium concentration LiFePO$_4$ particles	[18]
$c_{f,max}$	25677	[mol/m^3]	Max. lithium concentration carbon fibres	[24]

Table A1: Assumed model properties.

REFERENCES

[1] J.T. South, R.H. Carter, J.F. Snyder, C.D. Hilton, D.J. O'Brien and E.D. Wetzel, Multifunctional Power-Generating and Energy Storing Structural Composites for U.S. Army Applications, *Proceedings of the 2004 MRS Fall Conference*, Boston, MA, 851, 2004, pp. 2.1-2.13.

[2] S. Ekstedt, M. Wysocki and L.E. Asp "Structural batteries made from fibre reinforced composites". *Plastics, Rubber and Composites*, **39**, 2010, pp. 148–150 (doi: 10.1179/174328910X12647080902259).

[3] T. Carlson, *Multifunctional composite materials – design, manufacture and experimental characterisation*, Doctoral Thesis, Luleå University of Technology, Sweden, 2013.

[4] L.E. Asp and E. Greenhalgh, Structural power composites, *Composite Science and Technology*, **101**, 2014, pp. 41–61 (doi: 10.1016/j.compscitech.2014.06.020).

[5] L.E. Asp, A. Bismarck, T. Carlson, G. Lindbergh, S. Leijonmarck and M. Kjell, *A battery half-cell, a battery and their manufacture (structural battery)*, PCT, Patent No. 2893582, November 16th 2016. (Intl Appl No. PCT/EP2013/068024, 2013).

[6] G. Fredi, S. Jeschke, A. Boulaoued, J. Wallenstein, M. Rashidi, F. Liu, R. Harnden, D. Zenkert, J. Hagberg and G. Lindbergh, Graphitic microstructure and performance of carbon fibre Li-ion structural battery electrodes, *Multifunctional Materials*, **1**, 2018, 015003 (doi: 10.1088/2399-7532/aab707).

[7] M.H. Kjell, E. Jacques, D. Zenkert, M. Behm and G. Lindbergh, PAN-based carbon fiber negative electrodes for structural lithium-ion batteries, *Journal of Electrochemical Society*, **158**, 2011, pp. A1455–A1460 (doi: 10.1149/2.053112jes).

[8]   W. Johannisson, N. Ihrner, D. Zenkert, M. Johansson, D. Carlstedt and L.E. Asp, Multifunctional properties of a carbon fiber UD lamina structural battery electrode, *Composite Science and Technology*, **168**, 2018, pp. 81–87 (doi: 10.1016/j.compscitech.2018.08.044).

[9]   J. Xu, G. Lindbergh and J. Varna, Carbon fiber composites with battery function: Stresses and dimensional changes due to Li-ion diffusion, *Journal of Composite Materials*, **52**, 2018, pp. 2729–2742 (doi: 10.1177/0021998317752825).

[10]   J. Xu, G. Lindbergh and J. Varna, Multiphysics modeling of mechanical and electrochemical phenomena in structural composites for energy storage: Single carbon fiber micro-battery, *Journal of Reinforced Plastic Composites*, **37**, 2018, pp. 701–715, (doi: 10.1177/0731684418760207).

[11]   D. Carlstedt, E. Marklund and L.E. Asp, Effects of state of charge on elastic properties of 3D structural battery, *Composite Science and Technology*, **169**, 2019, pp. 26–33, (doi: 10.1016/j.compscitech.2018.10.033).

[12]   D. Carlstedt and L.E. Asp, Thermal and diffusion induced stresses in a structural battery under galvanostatic cycling, *Composite Science and Technology*, **179**, 2019, pp. 69-78, (doi: 10.1016/j.compscitech.2019.04.024).

[13]   M. Doyle, T.F. Fuller and J. Newman, Modeling of Galvanostatic Charge and Discharge of the Lithium/Polymer/Insertion Cell, *Journal of Electrochemical Society*, **140**, 1993, pp. 1526-1533 (doi: 10.1149/1.2221597).

[14]   J. Newman and W. Tiedemann, Porous-electrode theory with battery applications, *AIChE Journal*, **21**, 1975, pp. 25-41 (doi: 10.1002/aic.690210103).

[15]   R.E. Garcia, Y.M. Chiang, W.C. Carter, P. Limthongkul and C.M. Bishop, Microstructural modeling and design of rechargeable Lithium-ion batteries, *Journal of Electrochemical Society*, **152**, 2005, pp. A255–A263 (doi: 10.1149/1.1836132).

[16]   H. Arunachalam, S. Onori, I. Battiato, On Veracity of Macroscopic Lithium-Ion Battery Models, *Journal of Electrochemical Society*, **162**, 2015, pp. A1940–A1951 (doi: 10.1149/2.0771509jes).

[17]   E. Jacques, M.H. Kjell, D. Zenkert and G. Lindbergh, The effect of lithium-intercalation on the mechanical properties of carbon fibres, *Carbon N. Y.,* **68**, 2014, pp. 725–733 (doi: 10.1016/j.carbon.2013.11.056).

[18]   Y. Qi, L.G. Hector, C. James and K.J. Kim, Lithium Concentration Dependent Elastic Properties of Battery Electrode Materials from First Principles Calculations, *Journal of Electrochemical Society*, **161**, 2014, pp. F3010–F3018 (doi: 10.1149/2.0031411jes).

[19]   D.A.G. Bruggeman, Berechnung verschiedener physikalischer Konstanten von heterogenen Substanzen. I. Dielektrizitätskonstanten und Leitfähigkeiten der Mischkörper aus isotropen Substanzen, *Annalen der Physik*, **24**, 1935, pp. 636-664 (doi: 10.1002/andp.19354160705)

[20]   A.R. Melro, P.P. Camanho and S.T. Pinho, Influence of geometrical parameters on the elastic response of unidirectional composite materials, *Composite Structures*, **94**, 2012, pp. 3223-3231 (doi: 10.1016/j.compstruct.2012.05.004).

[21]   W.B. Gu and C.Y. Wang, Thermal-Electrochemical Modeling of Battery System, *Journal of Electrochemical Society*, **147**, 2000, pp. 2910-2922 (doi: 10.1149/1.1393625).

[22]   N. Ihrner, W. Johannisson, F. Sieland, D. Zenkert, M. Johansson, Structural Lithium Ion Battery Electrolytes via Reaction Induced Phase-Separation, *Journal of Material Chemistry A*, **5**, 2017, pp. 25652–25659 (doi: 10.1039/C7TA04684G).

[23]   K. Xu, Nonaqueous liquid electrolytes for lithium-based rechargeable batteries, *Chemical Review*, **104**, 2004, pp. 4303–4417 (doi: 10.1021/cr030203g).

[24]   M.H. Kjell, T.G. Zavalis, M. Behm and G. Lindbergh, Electrochemical Characterization of Lithium Intercalation Processes of PAN-Based Carbon Fibers in a Microelectrode System, *Journal of Electrochemical Society*, **160**, 2013, pp. A1473–A1481 (doi: 10.1149/2.054309jes).